Available online at www.sciencedirect.com

ScienceDirect

Procedia Structural Integrity 49 (2023) 10–15

Structural Integrity Procedia

www.elsevier.com/locate/procedia

Medical Devices: Materials, Mechanics and Manufacturing

M3D-BIO - Microfluidics-Enabled 3D Printing for Biofabrication

Amirpasha Moetazedian[a,b]*, Alessia Candeo[c], Andrea Bassi[c], Liam R. Cox[d], Liam M. Grover[e], Gowsihan Poologasundarampillai[a]

[a]*School of Dentistry, University of Birmingham, Birmingham, B5 7EG, UK*
[b]*EPSRC Future Metrology Hub, School of Computing and Engineering, University of Huddersfield, Huddersfield, HD1 3D, UK*
[c]*Dipartimento di Fisica, Politecnico di Milano, Piazza Leonardo da Vinci 32, Milano, 20133 Italy*
[d]*School of Chemistry, University of Birmingham, Edgbaston, Birmingham, B15 2TT, UK*
[e]*School of Chemical Engineering, University of Birmingham, Edgbaston, Birmingham, B15 2TT, UK*

Abstract

Microfluidics market is the fastest growing research area in the world, and they have shown much promise in biofabrication and 3D bioprinting of tissues and organs. However, microfluidics is conventionally produced using drawn-out and expensive lithographic methods, hindering their wider uptake. To this end, we have established a streamlined pipeline which incorporates simulation, design, fabrication and validation processes to produce versatile microfluidic chip nozzles for a range of applications in biofabrication. The microfluidic devices are produced by combining material extrusion additive manufacturing (MEAM) with innovative design approaches to achieve leak-free and low-surface roughness channels without any need of special tubing. These microfluidic chip nozzles create complex anisotropic fibrous core-shell structures matching blood vessels at resolutions not reported previously. The results of this study show that the novel microfluidics system can be adopted in a wide range of applications from tissue scaffolds, cell culture systems, biochemical sensors and lab-on-a-chips, paving ways for next generation of 3D-printed microfluidics in biofabrication.

Keywords: Additive Manufacturing; Microfluidics; Fluid mixing; Regenerative medicine

* Corresponding author. Tel.: +44 1484 258852.
E-mail address: a.moetazedian@hud.ac.uk

10.1016/j.prostr.2023.10.003

1. Introduction

Next generation, non-animal technologies have the potential to replace *in vivo* animal models in bioscience research. Complex 3D tissue models are one of several technologies anticipated to deliver this potential. Due to its speed, accuracy and versatility, 3D-bioprinting is showing much promise in producing artificial tissues (Moetazedian et al. 2022). However, key challenges need to be addressed before 3D-bioprinting can fulfill its potential. These include: (i) inability to reproduce tissue hierarchy below 100 μm (Fig. 1a); and (ii) mechanical damage on cells during bioprinting. Cells experience shear and extensional force during extrusion bioprinting, leading to 10-60% of the printed cells undergoing necrosis depending on the extrusion process. Thus, success depends on preventing or minimising mechanical cell damage. To overcome these issues, microfluidics-enabled 3D bioprinting has been explored as a smarter printing strategy.

Microfluidic devices are normally produced from polydimethylsiloxane (PDMS), due to its affordability, biocompatibility for implantable devices (Au et al 2014). The process is well-known (Gale et al 2018, Kim et al. 2008) and involves a series of manufacturing processes, making it expensive, time-consuming, resource-heavy and difficult for wider adoption (Gale et al 2018, Kim et al. 2008, Guerra et al. 20018). All of this drives the costs high, with individual chips costing more than $200 (Gale et al 2018, Kim et al. 2008, Guerra et al. 20018). With increasing emphasis on translation and low-cost microfluidic devices, such fabrication methods are facing a '*manufacturability roadblock*' (Bhattacharjee et al. 2016).

Additive manufacturing (AM) platforms offer an exciting solution to overcoming this manufacturing roadblock. AM is transforming research and industrial sectors thanks to its capacity to fabricate bespoke parts rapidly and reproducibly with intricate geometries (Moetazedian et al. 2021). In recent years, AM technologies have gained considerable investment from the healthcare sector as they enable the development of drug-delivery devices, patient-specific implants, and 3D in vitro tissue models. With latest developments in custom toolpaths for AM, there has been new opportunities to explore the production of high-value 3D-printed parts such as microfluidic devices (Gleadall 2021, Quero et al 2021). Of AM technologies, material extrusion additive manufacturing (MEAM) is the most affordable, that makes it an ideal option for manufacturing readily-accessible microfluidic devices (Lee at al. 2014). However, the state-of-the-art MEAM microfluidics suffer from low optical transparency, low resolution, difficulties in achieving leak-free structures, poor surface finish ($R_a \approx 10.9$ μm vs 0.35 μm for laser-based AM) and limited capabilities to create complex structures, which is limiting their application and translation (Macdonald et al. 2017). To tackle these challenges, we have developed a novel 3D bioprinting workflow (Moetazedian et al. 2023) employing 3D-printed microfluidic chips to produce complex structures (Fig. 1b). Our microfluidic chips integrate microfluidic mixers and hydrodynamic flow focusing components to simultaneously deliver various hydrogels and cells through a narrow nozzle. The fluidic chips enable extrusion of complex architectures including core-shell and multi-material fibres (Fig. 1c).

Nomenclature

ABS	Acrylonitrile butadiene styrene
AM	Additive Manufacturing
FDM	Fused deposition modelling
FFF	Fused filament fabrication
MEAM	Material Extrusion Additive Manufacturing
PDMS	Polydimethylsiloxane

2. Methodology

White Acrylonitrile butadiene styrene (ABS) filament (Rasie3D® Premium ABS) with 1.75 mm diameter was used to manufacture microfluidic channels using a Creality Ender 3 V2 machine. Sylgard® 184 and its curing agent (PDMS, Dow Corning) was used as a matrix to embed the ABS channels. The nozzle's temperature was set at 240°C to extrude

a continuous single layer of ABS filaments as shown in Fig. 1b. Custom GCode commands (series of commands controlling the MEAM printer) were generated using an open-source FullControl GCode designer software (Gleadall 2021). Four passive mixer designs were manufactured and named as follows: zigzag (for constant-width zigzag, Fig. 1b[iv]), V-zigzag (for variable-width zigzag, Fig. 1b[iv]), hex (for hexagonal mixer, Fig. 1b[iv]), and diamond. To achieve co-axial hydrodynamic flow focusing of calcium chloride-Pluronic solution (bioink 1) by 2 wt% sodium alginate solutions (bioink 2), the calcium chloride channel had a smaller diameter (0.4 mm) than sodium alginate channels (1.0 mm). The manufactured channels (Fig. 1a) were selectively exposed to a droplet of acetone for 10 s to remove the surface roughness caused by nozzle movements. The ABS channels were cast PDMS before flushing with acetone (Fig. 1b). Sodium alginate and calcium chloride-Pluronic were pumped through the channel at flow rates ranging from 500 to 2000 µl.min^{-1}. The scanning electron microscopy (SEM) was used to assess the 3D-printed fibres (Fig. 1c).

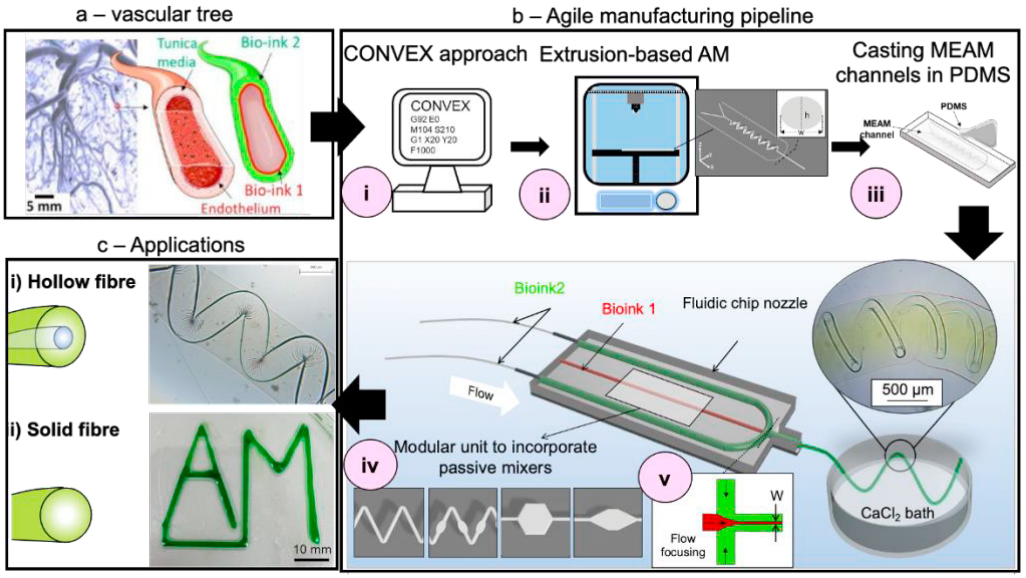

Fig. 1 To recreate natural blood vessel (a), a novel microfluidic chip nozzle for extrusion printing platform was developed to recapitulate the heterogeneity of blood vessel (b-c). The potential applications including but not limited to: (i) fabrication of anisotropic multi-layer structures with defined diameters and shapes; and (ii) reactive mixing (c).

3. Results and discussion

3.1. Surface roughness characterisation of channels

The surface roughness (R_a) of the MEAM channels was quantified in two directions, namely along the fluid flow and perpendicular to direction of the fluid flow to investigate the effect of direction on these measurements before and after acetone treatment. Before acetone treatment, the hex and diamond designs had surface roughness values of 0.49 ± 0.11 µm and 0.92 ± 0.21 µm, respectively (Fig. 2a). These values were more than three times higher than values measured for the zigzag (0.15 ± 0.01 µm) and V-zigzag (0.16 ± 0.02 µm) designs. Furthermore, for the hex and diamond designs, the surface roughness was dependent on the direction of measurement. When measured normal to the fluid flow (Fig. 2b), values increased by 24.4% and 60.6% for hex and diamond, respectively, compared to the values measured along the fluid flow (Fig. 2b). These differences can be understood; for the diamond design, more filaments (4 lines) were needed to fill in the space compared to the Hex design (3 lines). Nevertheless, the hex mixer with the highest surface roughness value still showed over 85% lower surface roughness compared to those reported

previously (Macdonald et al. 2017). Such differences arise from the fact that in this study, a single layer of filament is deposited compared with the multi-layer channels in the literature.

The effect of acetone on the surface roughness was investigated by performing measurements of surface roughness along the direction of the fluid flow. The mean surface roughness for the hex, diamond, zigzag and V-zigzag designs were 0.16 ± 0.07 µm, 0.17 ± 0.05 µm, 0.13 ± 0.04 µm, 0.14 ± 0.02 µm, respectively, with no considerable variation ($p > 0.05$) between them. Similar values were obtained when surface roughness was measured perpendicular to the fluid flow for the hex and diamond designs (0.15 ± 0.05 µm and 0.17 ± 0.03 µm, respectively), with only 6.4% difference between the two directions. These results demonstrate how acetone treatment reduces surface roughness of the MEAM channels by removing the texture in both directions, creating a flat featureless surface topography, comparable to those produced by injection moulding (Tosello et al 2012). The calculated surface roughness in this study was impressively lower (up to 98.7% reduction) than the values reported in the literature for similar MEAM specimens (McDonald et al 2002).

These findings are substantial since one of the major limitations of MEAM for fabrication of microfluidic devices is poor surface finish, which has been reported to limit the optical performance of microfluidics (McDonald et al 2002) and ultimately result in cell sedimentation (Ali 2021). We have addressed this issue by combining the manufacturing strategy (i.e., printing single layer) with an operationally practical acetone treatment. The finished MEAM microfluidic devices were visibly transparent due to the use of PDMS as the matrix (Figure 6c). Optical transparency is important for certain applications where high-resolution imaging of the channels, including light-sheet microscopy (Poologasundarampillai et al. 2021), is necessary to track fluid flow through the channels. A series of images captured at the tip of the nozzle (Fig. 2c) were used to examine the smoothness of the channels. All images reveal smooth walls with no indication of ridges or texture, supporting the surface roughness data (Fig. 2a-b). Acetone-treated channels were therefore used for the rest of the study.

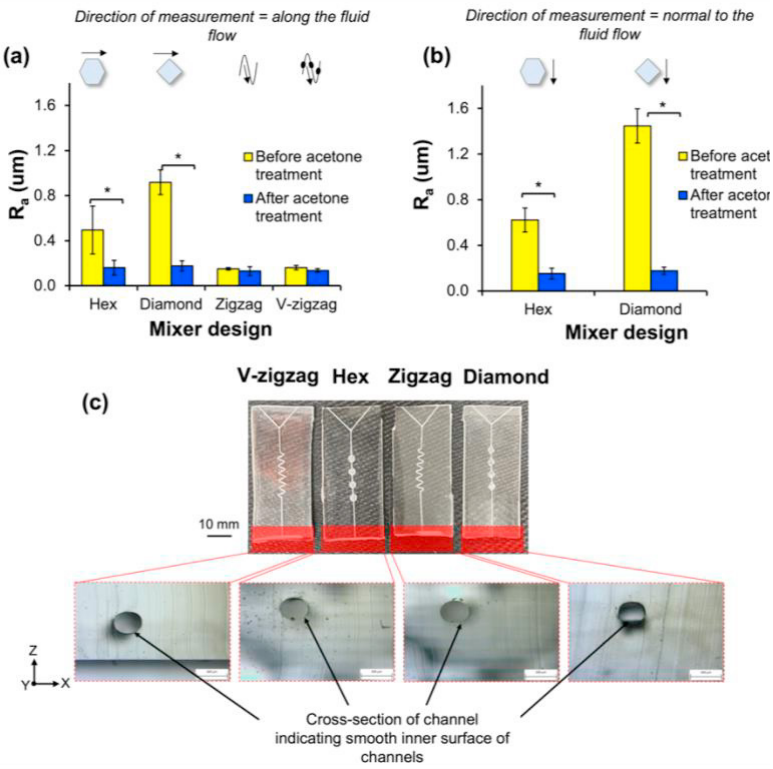

Fig. 2 Mean surface roughness (R_a) values measured for all four designs (a) along and (b) normal to the fluid flow. (c) Images after ABS dissolution, revealing smooth channel walls, similar to those produced by lithography. The MEAM microfluidic after dissolving the ABS channels with acetone significantly (* $p < 0.05$) improved the surface roughness for the hex and diamond designs in both directions. For the zigzag and V-zigzag designs, the surface roughness improved but not significantly ($p > 0.05$). Mean values calculated from 3 replicates.

3.2. Microfluidic-enabled 3D bioprinting for biofabrication

Microfluidic nozzles offer spatiotemporal control over the printing process, enabling recreation of the structural complexity of native tissues. To date, most commercially available microfluidic printheads are produced using conventional lithography methods. Here, a MEAM microfluidic chip nozzle, capable of controlling the diameter of a deposited fibres by flow-focusing (Fig. 3a-b) has been produced. To this end, 2 wt% sodium alginate and calcium chloride-Pluronic solutions were prepared with yellow and blue dye, respectively (Fig. 3a). The flow-focusing component allowed the core fluid ($CaCl_2$-Pluronic) to be concentrated inside the microfluidic channel between the sodium alginate layers introduced either side of the core. Contact-gelation of sodium alginate happened by divalent cationic crosslinking at the interface between the two fluids, while the majority of the sodium alginate remined as solution and was only crosslinked once extruded into a 10 wt% $CaCl_2$ bath. After extrusion, the core fluid is removed to give hollow fibers (Fig. 3c-d). By systematically varying the flow rates of core and shell, a range of core architectures (straight, wavy and helical) could be produced (Fig. 3d) with varying fiber widths. To confirm the printed fibres were hollow, SEM micrographs of fibres were obtained (Fig. 3e-g), highlighting the surface texture of fibres as well as demonstrating the core layer is hollow (Fig. 3f).

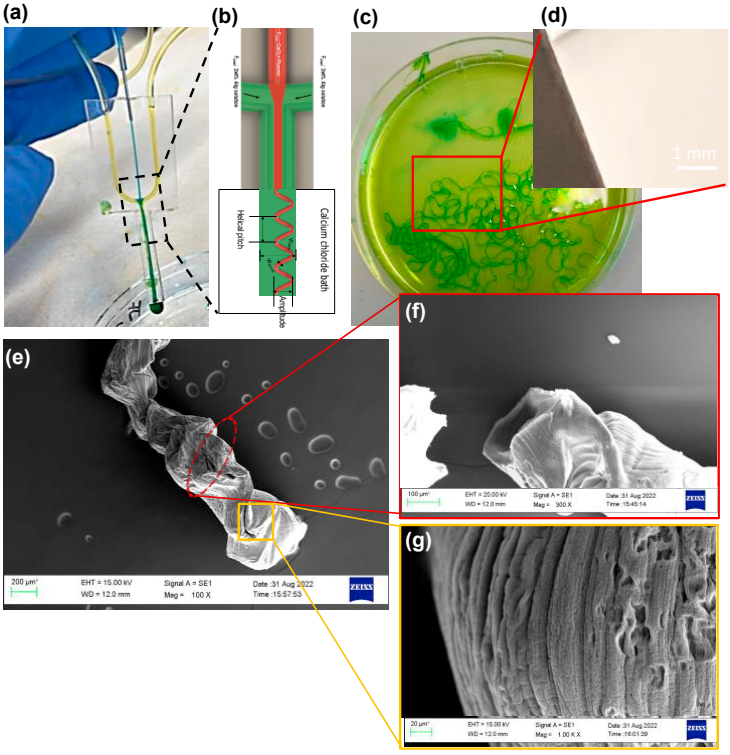

Fig. 3 3D-printed microfluidic chip nozzle (a) containing flow focusing components (b). The newly devised microfluidic chip nozzle enables hydrogel in-situ gelation and flow focusing to produce high-resolution core-shell fibres mimicking blood vessels (c-d). SEM micrographs of extruded fibres indicating the surface texture and the hollow core layer (e-g).

4. Conclusions

Our nimble microfluidic chip nozzles were fabricated using an expensive MEAM machine from ABS to assess their suitability as a viable option to enable wider uptake of microfluidics. The results showed that by direct control of the 3D printer process and a simple acetone treatment, it was possible to produce complex, seamless and low-surface roughness channels comparable to lithographic-microfluidics. Our nimble microfluidic chip nozzles enable fluid mixing and manipulation leading to fabrication of complex fibrous structures. The 3D-printed microfluidic chip

nozzles manufacturing requires less than 1/50 of the resources compared to the traditional microfluidic manufacturing. The state-of-the art core-shell fibres are the first to match the scale and architecture of spiral arterioles that play a key role in metabolite and oxygen transport. The novel 3D-printed microfluidic chip nozzle is expected to enable new opportunities in biofabrication.

Acknowledgements

The authors thank EPSRC (grant number EP/V051342/1) for funding to G.P. and A.M.

References

Ali, D. 2021. Influence of Cell Transportation Microchannel Wall Quality on Cell Deposition Risk: a DPM Analysis, in: Int. Conf. Sci. Technol. Eng. Sci. Technol.

Gale, B.K et al. 2018, A review of current methods in microfluidic device fabrication and future commercialization prospects, Inventions. 3: 3030060.

Gleadall, A. 2021 FullControl GCode Designer: open-source software for unconstrained design in additive manufacturing., Addit. Manuf. 46: 102109.

Guerra, M.G, Volpone, C, Galantucci, L.M, Percoco, G. 2018. Photogrammetric measurements of 3D printed microfluidic devices, Addit. Manuf. 21: 53–62

Kim, P. et al. 2008. Soft lithography for microfluidics: A Review, Biochip J. 2: 1–11.

Lee, K.G. et al. 2014. 3D printed modules for integrated microfluidic devices, RSC Adv. 4: 32876–32880.

Macdonald, N.P, Cabot, J.M, Smejkal, P, Guijt, R.M, Paull, B, Breadmore, M.C. 2017. Comparing Microfluidic Performance of Three-Dimensional (3D) Printing Platforms, Anal. Chem. 89:3858–3866.

McDonald, J.C, Chabinyc, M.L, Metallo, S.J, Anderson, J.R, Stroock, A.D, Whitesides, G.M. 2002. Prototyping of microfluidic devices in poly(dimethylsiloxane) using solid-object printing, Anal. Chem. 74:1537–1545

Moetazedian, A. et al. 2022 Convex microfluidic devices: A new microscale agile manufacturing pipeline for material extrusion additive manufacturing. Eng. Arch.

Poologasundarampillai, G, Haweet, A, Jayash, S.N, Morgan, G, Moore, J.E., Candeo, A. 2021. Real-time imaging and analysis of cell-hydrogel interplay within an extrusion-bioprinting capillary, Bioprinting. 23: e00144.

Quero, R.F, Domingos da Silveira, G, Fracassi da Silva, J.A, De Jesus, D.P. 2021. Understanding and improving FDM 3D printing to fabricate high-resolution and optically transparent microfluidic devices, Lab Chip 21: 3715-3729.

Tosello, G, Marinello, F, Hansen, H.N. 2012. Characterisation and analysis of microchannels and submicrometre surface roughness of injection moulded microfluidic systems using optical metrology, Plast. Rubber Compos. 41: 29–39.